energies

MDPI

Article

Effect of Agitator Operating Parameters on Biogas Yield and Process Stability in a Full-Scale Dry Anaerobic Digester

Przemysław Seruga [1,*], Wojciech Czekała [2,*], Marta Wilk [1], Agnieszka Urbanowska [3] and Mateusz Jackowski [4]

[1] Department of Bioprocess Engineering, Faculty of Production Engineering, Wrocław University of Economics and Business, Komandorska 118/120, 53-345 Wrocław, Poland; marta.wilk@ue.wroc.pl
[2] Department of Biosystems Engineering, Poznań University of Life Sciences, Wojska Polskiego 50, 60-627 Poznań, Poland
[3] Department of Water, Wastewater and Waste Technology, Faculty of Environmental Engineering, Wrocław University of Science and Technology, Wyb. Wyspiańskiego 27, 50-370 Wrocław, Poland; agnieszka.urbanowska@pwr.edu.pl
[4] Department of Micro, Nano and Bioprocess Engineering, Faculty of Chemistry, Wrocław University of Science and Technology, Norwida 4/6, 50-373 Wrocław, Poland; mateusz.jackowski@pwr.edu.pl
* Correspondence: przemyslaw.seruga@ue.wroc.pl (P.S.); wojciech.czekala@up.poznan.pl (W.C.)

Abstract

Mixing is one of the largest single consumers of parasitic electricity in a biogas plant. Yet, the quantitative effect of agitator operation on performance has been established almost exclusively at laboratory or pilot scale, and rarely for dry digestion. Unlike previous full-scale studies, which varied only the duration of mixing in mostly wet digesters, this study varied agitator rotational speed, run time, and pause time jointly (three levels each; a Taguchi L9 design run in two series, 18 runs in total) on an operating municipal dry (32–35% TS) horizontal-shaft digester treating source-segregated biowaste, with three-point (inlet/middle/outlet) pulp analyses. Specific biogas yield ranged from 71 to 106 m^3/Mg across the nine settings. Analysis of variance identified rotational speed as the dominant factor ($p < 0.001$); yield increased monotonically with speed, most strongly between 0.2 and 0.4 rpm (yield = 68.0 + 50.2·speed[rpm], $R^2 = 0.64$, $p < 0.001$). The yield-maximizing combination within the tested range (0.6 rpm; 400 s run; 150 s pause) increased biogas yield by 37% relative to the pre-experiment settings, and a confirmation run (104.4 m^3/Mg) agreed with the additive-model prediction (105.1 m^3/Mg). Because the mixing-energy index, which combines torque, speed, and duty cycle, was also highest at this setting, the yield-maximizing and energy-efficient operating points differ. The digester remained stable throughout (outlet FOS/TAC 0.13–0.17; over 98% net decrease in acetic acid from inlet to outlet), so the yield differences were not associated with acidification.

Keywords: anaerobic digestion; dry fermentation; source-segregated biowaste; mixing; agitator speed; biogas yield; full-scale

Check for updates

Academic Editor: Prasad Kaparaju

Received: 28 September 2026
Revised: 11 October 2026
Accepted: 26 October 2026
Published: 28 October 2026

Copyright: © 2026 by the authors. Licensee MDPI, Basel, Switzerland. This article is an open access article distributed under the terms and conditions of the Creative Commons Attribution (CC BY) license.

1. Introduction

Anaerobic digestion (AD) of source-segregated biowaste, including food waste, is a central technology for coupling municipal waste management with renewable-energy recovery, converting biodegradable waste into biogas while stabilizing the residual digestate for agricultural use [1,2]. Beyond energy recovery, AD is one of the main pathways through which the biogenic carbon and nutrients of municipal waste are recovered—as methane, and as digestate that returns organic carbon and nutrients to soil [2]—so improving its efficiency

contributes directly to circular carbon and resource-recovery strategies. The efficiency of a biogas plant is determined by both the amount of methane it produces and the fraction of that energy it consumes internally [3,4]. Among internal consumers, mixing is one of the most significant: in full-scale plants, the mixing system can account for a large share of on-site electricity use [3,5], and inadequate mixing is a frequent cause of sedimentation, floating layers, and foaming [6,7].

Mixing fulfills several competing functions. It disperses fresh feedstock, distributes heat, releases entrapped biogas, and prevents stratification. Still, excessive agitation imposes hydrodynamic shear that disrupts the flocs within which syntrophic bacteria and methanogens exchange intermediates and has repeatedly been linked to depressed methane production and propionate accumulation [8,9]. A broad body of laboratory and review work now converges on the view that vigorous, continuous mixing should be avoided and that gentle, intermittent regimes are both more productive and more energy-efficient [8,10,11]. At the process level, intermittent mixing has been shown to increase biogas yield relative to continuous mixing in manure [12] and in the organic fraction of municipal solid waste (OFMSW) [8]. In an intermittently mixed vinasse digester, biogas production increased with mixing speed (20–60 rpm) but became less stable at the highest speed [13]. Conversely, excessively long agitation intervals allow a floating layer to form, thereby reducing yield [6].

Two aspects of a mixing regime are usually distinguished: the intensity of agitation (rotational speed) and its temporal pattern (mixing duration and the length of the resting interval between mixing) [14]. Both have been studied, but almost always separately and at a small scale. Speed and shear effects have been quantified in bench reactors [9,15,16]. Intermittent-mixing intervals have been optimized in liter-scale digesters, where lengthening the resting interval from 1 h to 2–4 h reduced biogas yield by about 5–12% [14], and, in the digestion of corn stover at the highest loading rate tested, a 12 h agitation interval reduced the biogas production rate by about 29% relative to a 2 h interval because a floating layer formed [6]. Food waste and co-digestion studies at laboratory scale similarly report higher yields at lower mixing intensity [17,18].

A further, under-recognized complication is the solids content of the digesting mass. Most of the mixing literature concerns wet systems (total solids (TS) about 10%), whereas a large and growing share of OFMSW is treated by dry digestion at TS of roughly 20–40%, in commercial horizontal plug-flow systems that rely on a slow internal agitator to prevent sedimentation [1]. The rheology of a 30% TS mass is radically different from that of a dilute slurry: yield stress and viscosity rise steeply and non-linearly with TS, mixing becomes markedly more energy-intensive, and mass-transfer limitation rather than kinetic limitation often controls performance [1,19,20]. Optima obtained in wet, stirred-tank reactors, therefore cannot be assumed to transfer to a high-solids horizontal-shaft digester.

Evidence at full scale is scarce and is dominated by tracer or nutrient-distribution studies that characterize mixing quality rather than its effect on yield [21,22]. The few full-scale performance studies are nonetheless encouraging: at a large agricultural biogas plant, combined temperature and stirring management raised the specific electricity yield by 11.7% and reduced internal energy consumption by 10.4% [4], consistent with laboratory evidence that intermittent mixing (2 h on, 1 h off) can save about 29% of the mixing power with no yield penalty [23]. These results suggest that the small-scale consensus broadly holds at full scale. Still, they treat the timing of mixing in isolation, do not account for the joint effect of speed and timing, are almost all from wet systems, and do not pair yield with a concurrent, spatially resolved assessment of process stability. At full scale, such comparisons are further complicated by uncontrolled variability in feedstock composition, loading, and reactor history, which makes replicated designs and an explicit treatment of uncertainty necessary. As several researchers emphasize, mixing outcomes are strongly

system-specific—depending on agitator and digester geometry, slurry rheology, organic loading, and retention time—so an optimum obtained in one reactor does not transfer directly to another [10,11,24].

The present study directly addresses this gap. Its novelty is fourfold. First, the experiment is performed on a full-scale, operating municipal biowaste digester under normal production conditions. Second, and distinctively, the reactor is a high-solids (32–35% TS) horizontal-shaft system, a configuration for which quantitative mixing-optimization data are essentially absent, so the study probes the mixing–rheology interaction in the regime where it matters most. Third, three agitator parameters—rotational speed, run time, and pause time—are varied simultaneously within a single orthogonal design, allowing their relative influence to be ranked in a single campaign rather than inferred across incompatible single-factor studies. Fourth, each trial couples operational yield with an indicator of mixing energy (agitator torque combined with rotational speed and duty cycle) and a three-point pulp-stability profile, so that changes in yield can be examined together with mixing energy and process stability. This study aims to determine whether agitator settings measurably influence yield and stability in a full-scale high-solids digester, identify the controlling parameter, and distinguish the yield-maximizing operating point from energy-efficient operating points for this reactor class.

2. Materials and Methods

2.1. Full-Scale Digester and Feedstock

The experiment was conducted at an operating municipal biogas plant treating source-segregated biowaste, including food waste. The plant is a dry digestion system comprising two parallel horizontal plug-flow chambers; the experiment was conducted in one of them, which has a total volume of 1500 m^3 and was operated at a mean working volume of approximately 1230 m^3. The chamber is agitated by a single low-speed horizontal shaft that runs the full length of the vessel and is supported at both ends. Digestion was thermophilic, with the reactor temperature maintained at 54 ± 0.2 °C; the biogas methane content was stable at about 54 ± 0.3% (v/v). The digesting mass was in the high-solids range, with total solids of 32–35%, classifying the system as dry anaerobic digestion and necessitating the use of this horizontal agitator shaft rather than a submersible or gas-mixing device.

The agitator consists of a horizontal shaft carrying radial star-shaped arms that run the full length of the chamber, sweeping a circle with a diameter of 6.64 m, corresponding to an effective swept radius of 3.32 m. The lower and lateral arms are fully submerged in the digesting mass. At the same time, the upper part of the swept circle passes through the gas–liquid interface, so the agitator acts on the bulk by kneading the high-solids matrix rather than by shearing a dilute suspension.

Feeding was quasi-continuous, in evenly distributed cycles of approximately 1 Mg each; the mean daily feedstock mass of the individual runs ranged from 38.0 to 46.7 Mg/d (Section 3.1). Because the mixing regime, not the load, was the object of study, the primary response was normalized to the feedstock mass and expressed as the specific biogas yield (m^3/Mg).

2.2. Experimental Design

Three agitator operating parameters were investigated at three levels each: rotational speed (X1), run time (X2), and pause time (X3). An orthogonal array was adopted, reducing the full factorial (27 runs) to nine industrial trials while preserving orthogonal, balanced coverage of the factor space. The factor levels are given in Table 1, and the design matrix is given in Table 2. Coded levels (−1, 0, +1) are used throughout the analysis. A reference

run (T0), corresponding to the pre-experiment plant settings (0.25 rpm, 350 s run, 150 s pause), was recorded for benchmarking but excluded from the orthogonal analysis.

Table 1. Investigated factors and their levels.

Factor	Unit	Level −1	Level 0	Level +1
X1—rotational speed	rpm	0.2	0.4	0.6
X2—run time	s	100	250	400
X3—pause time	s	50	150	250

Table 2. Coded factor levels of the design matrix.

Trial	X1	X2	X3
1	+1	−1	−1
2	+1	0	+1
3	+1	+1	0
4	0	−1	+1
5	0	0	0
6	0	+1	−1
7	−1	−1	0
8	−1	0	−1
9	−1	+1	+1

Given the effective (swept) radius of 3.32 m, the three tested rotational speeds (0.2, 0.4, and 0.6 revolutions per minute (rpm)) correspond to arm-tip linear velocities of approximately 7.0, 13.9, and 20.9 cm/s, respectively. Expressing the speed in these terms allows direct comparison with high-solids studies that report agitation in terms of linear velocity rather than rpm.

2.3. Operational Data and Pulp Analyses

Each run was operated at a fixed set of agitator settings for a continuous period, and the operational indicators were averaged over that period. To limit carry-over effects from the preceding mixing regime, each parameter change was followed by a transition period of at least 7 days, which was excluded from the evaluation. Because this transition period is shorter than the HRT (about 27–33 days), the digester content was not fully exchanged between runs; the agitator, however, acts mainly on the hydrodynamic state of the digesting mass (substrate–biomass contact and release of entrapped gas) rather than on its composition, so its effect on gas production is expected to become apparent within days. Furthermore, source-segregated biowaste contains a large fraction of readily biodegradable organics that are rapidly converted [1,20], so the gas production from the most active substrate fraction is expected to respond to changes in mixing within days. The 7-day period was, however, treated only as a minimum. Data collection for a given run was initiated only after the online biogas production rate had reached a plateau without systematic drift, i.e., when the daily biogas production remained within ±10% of its running mean for at least 6 consecutive days without a monotonic trend, a criterion adapted from Tian et al. [6]; the outlet FOS/TAC ratio and individual VFAs, determined on pulp samples during each run, confirmed stable operation (Section 3.4). The following were logged from the plant control system: total and daily biogas production (m^3, m^3/d), methane content (%), total and daily feedstock mass (Mg, Mg/d), mean digester filling level (m^3), and the agitator torque (%). Agitator torque, reported by the drive as a percentage of nominal load, was recorded by the plant SCADA system as the maximum value in each run (the running time of the agitator was not logged separately); this maximum torque was combined with

the rotational speed and the duty cycle to estimate the relative mixing energy of each setting (Section 2.4). The specific biogas yield (m^3/Mg) was computed as the total biogas divided by the total feedstock mass of the run. To enable comparison with the anaerobic-digestion literature, in which specific yield is most often reported per unit of organic matter, the total solids (TS) and volatile solids (VS) of the feedstock were also determined gravimetrically according to Standard Methods [25]: TS as the residue after drying at 105 °C, and VS as the mass lost on ignition at 550 °C. The experiment was conducted on the continuously operating full-scale digester without interrupting production; the complete campaign, including transition periods, lasted approximately 10 months. The two replicate series were run as separate, non-adjacent operating periods under the same nine settings. Within each series, the nine settings were not applied in the order of the trial numbers; the sequence was chosen by the plant operator rather than by a formal randomization procedure, and the exact order was not recorded in the operational data made available to the authors. Temporal effects were limited by (a) running each series as a complete L9 array, so that a drift between the series acts as a block effect orthogonal to the factor effects (Section 2.4), (b) applying the settings in a non-sequential order, and (c) the transition period and steady-state criterion described above. Because the study uses a single production reactor, a replicate here denotes a separate operating period rather than an independent reactor, and the two series therefore also provide a measure of temporal reproducibility. Exact calendar dates are commercially restricted by the operator and are not disclosed; the structure of the campaign and the steady-operation criterion are, however, described here to ensure transparency.

The feedstock averaged 44.1 ± 10.4% TS and 72.5 ± 6.4% VS on a dry-mass basis, corresponding to a volatile-solids content of about 32% of the fresh mass. Because these characteristics were measured on the common feedstock rather than per individual trial, a single mean TS and VS value was applied to all runs; the specific yield was then additionally expressed per unit of volatile solids (m^3/Mg VS). Feedstock TS and VS were determined on 18 composite samples collected at approximately two-week intervals throughout the campaign, independently of the run schedule, to track seasonal changes in feedstock composition; per-run values are therefore unavailable. Given the considerable variability of feedstock TS (coefficient of variation of about 24%), the amount of volatile solids actually fed may have differed between runs, so part of the variation in yield per unit fresh mass may reflect feedstock composition rather than mixing; this is examined in Section 3.1 and discussed as a limitation in Section 3.5. To assess repeatability and enable a formal analysis of variance, the entire nine-run design was carried out in two replicate series (separate operating periods) under the same settings, yielding 18 experimental runs in total. In addition, a separate confirmation run was performed at the predicted optimum settings (0.6 rpm, 400 s run, 150 s pause) to validate the model prediction.

Process stability was assessed from pulp samples taken at three positions along the chamber—inlet, middle, and outlet—using the dedicated sampling ports provided along the vessel. The following were determined: pH, total solids (TS, %), ammonium nitrogen (mgNH_4/kg), volatile fatty acids expressed as acidity (mgCH_3COOH/kg), alkalinity (mg$CaCO_3$/kg), the FOS/TAC ratio, and individual volatile fatty acids (VFAs) (acetic, propionic, butyric, iso-butyric, valeric, and iso-valeric acid; mg/kg). The inlet-to-outlet evolution of these variables characterized the net change in acid concentrations along the chamber and the reactor's buffering state.

Individual volatile fatty acids were determined by gas chromatography (Varian GC 450; Varian BV, Middelburg, The Netherlands) with a flame-ionization detector (FID; H_2: 30 mL/min, air: 300 mL/min, make-up He: 30 mL/min). Helium was the carrier gas at 1 mL/min with a 1:30 split ratio. Total solids, volatile solids, and pH were determined according to Standard Methods [25]. Ammonium nitrogen was determined by Hach tests

(LCK502, Hach Lange GmbH, Düsseldorf, Germany). Each parameter was measured on samples drawn at the inlet, middle, and outlet during each run.

2.4. Data Analysis

The influence of each operational factor was evaluated using the design of experiments, a widely adopted approach for optimizing anaerobic digestion with minimal experimental runs [26,27]. Rather than varying one factor at a time—which is prohibitively time-consuming at full scale and unable to resolve the relative importance of several factors—the Taguchi method distributes the factors across a balanced orthogonal array, allowing the main effect of each factor to be estimated efficiently from a fraction of the full-factorial runs [26,28]. For three factors at three levels, the L9 (3^3) array reduces the required experiments from 27 to 9 while preserving orthogonality; here, the full L9 design was carried out in two replicate series, giving 18 runs, so that experimental error could be estimated directly and the factor effects tested by analysis of variance. Within the array, each level of each factor is combined with each level of the other factors an equal number of times. Consequently, when the response is averaged over runs sharing a given level, the main effects of the remaining factors cancel out, so the effect of one factor is estimated uniformly across the varied levels of the others [26]. This balance, however, holds only if two-factor interactions are negligible. In the L9 array, interactions are partially aliased with the main effects and cannot be estimated separately [28], so the main effects reported here are averages over the other factors' levels. The balanced, fractional structure makes the design particularly suitable for a full-scale plant, where the number of settings that can be tested on a production digester is inherently limited. The specific biogas yield was treated as the primary response and analyzed under the "larger-the-better" criterion.

The larger-the-better signal-to-noise ratio, $S/N = -10 \cdot \log_{10}[(1/n) \cdot \Sigma(1/y_i^2)]$, was calculated for each setting from its two runs; it gave the same factor ranking and the same optimal levels as the level means of the yield (ranges of the S/N level means: speed 2.02 dB, pause time 0.95 dB, run time 0.49 dB), so the results are presented in terms of the yield itself. An additive model was utilized to predict the response at the theoretically optimum combination

$$R_{opt} = R_{av} + \sum(R_{level,\,opt} - R_{av}),$$

where R_{av} is the grand mean across all runs, and $R_{level,\,opt}$ is the mean response at the optimal level of each controlling factor.

Because the design was replicated, the experimental error could be estimated directly, and the significance of each factor was assessed by analysis of variance (ANOVA) on the eighteen runs, in addition to the Taguchi factor-means (Δ) analysis. Because both series were run in the same digester, they are repeated operating periods rather than independent reactors. As a conservative check that does not rely on the independence of the 18 runs, the nine setting means were also analyzed, using the unassigned column of the L9 array (2 df) as the error term; in addition, the residual of the 18-run ANOVA was partitioned into this column, which contains the aliased interactions, and the between-series pure error, to test the additive model for lack of fit [28]. A possible systematic difference between the two series was examined with a paired *t*-test over the nine settings and by including series as a block term in the ANOVA. Repeatability was quantified from the difference between the two replicate series, and the additive prediction at the optimum was verified against the independent confirmation run. The relationship between rotational speed and yield was further characterized using ordinary least squares linear regression and the Pearson correlation coefficient (r), with a two-tailed *p*-value ($\alpha = 0.05$). Residuals of the 18-run model were checked for normality (Shapiro–Wilk test) and homogeneity of variance (Levene's test across speed levels and Bartlett's test across settings); 95% confidence

intervals of the effects were calculated from the residual mean square, and a 95% prediction interval for the confirmation run from the variance of the additive prediction [28]. The relative mixing energy of each setting was expressed as

$$E_{rel} = (\tau/100) \cdot N \cdot t_{run}/(t_{run} + t_{pause}),$$

normalized to the yield-maximizing setting, where τ is the maximum torque recorded in the run (% of nominal; mean of the two series), N the rotational speed (rpm), and t_{run} and t_{pause} the run and pause times. Assuming that the torque during the running periods is proportional to this maximum, E_{rel} is proportional to the time-averaged shaft power and, at constant drive efficiency, to the electrical demand of the agitator.

3. Results and Discussion

3.1. Process Performance Across Runs

Across the campaign, the hydraulic retention time was approximately 27–33 days, and the organic loading rate was 9.7–12.0 kg VS/(m^3·d) (mean 11.1, coefficient of variation about 5%). Because the OLR was calculated with the common mean VS content, it reflects variation in feedstock mass only, not in feedstock composition. Feedstock mass, loading rate, and retention time for each run are reported in Table 3. The mean OLR of the two runs of each setting was not correlated with the mean specific yield of that setting ($r = 0.09$, $p = 0.81$, $n = 9$). The effect of speed remained significant when the OLR was included as a covariate (regression of the nine setting means on rotational speed with the mean OLR as covariate, $p = 0.003$); variation in feedstock mass is therefore unlikely to explain the yield differences, whereas variation in feedstock composition cannot be assessed with the available data.

Table 3. Operating data of all 18 runs (runs 1–9: first series, Trials 1–9; runs 10–18: second series, Trials 1–9).

Run	Feed (Mg/d)	Working Volume (m^3)	OLR (kg VS/(m^3·d))	HRT (d)
1	44.5	1232	11.56	28
2	46.7	1250	11.96	27
3	43.5	1248	11.15	29
4	42.8	1225	11.18	29
5	39.7	1227	10.35	31
6	38.0	1198	10.15	32
7	43.0	1215	11.33	28
8	46.2	1265	11.69	27
9	38.4	1264	9.72	33
10	42.9	1225	11.21	29
11	44.1	1237	11.41	28
12	44.5	1231	11.57	28
13	43.4	1232	11.27	28
14	42.6	1230	11.08	29
15	43.5	1241	11.22	29
16	41.4	1239	10.69	30
17	43.4	1237	11.23	29
18	43.6	1236	11.29	28

OLR = daily feed × TS × VS/working volume, calculated with the campaign means (TS = 44.1%, VS = 72.5% of TS); HRT = working volume/daily feed, assuming a bulk density of about 1 Mg/m^3.

The specific biogas yield varied substantially across the nine settings, from 71 to 106 m^3/Mg (Table 4), i.e., a 1.5-fold spread between agitator settings, obtained without

intentional changes to the feedstock or loading strategy (feedstock composition, however, varied naturally; Section 2.3). Relative to the pre-experiment reference (T0, 77.4 m^3/Mg), eight of the nine settings increased yield, with the best increasing by 37%. The methane content remained constant at about 54% in all trials, indicating that mixing affected the quantity of biogas produced rather than its quality—consistent with the view that in high-solids systems mixing governs the physical accessibility of substrate to the microbial community (i.e., mass transfer) rather than the metabolic pathway itself [1,29].

Table 4. Operational results for the nine settings (sorted by rotational speed).

Trial	X1 (rpm)	X2 (s)	X3 (s)	Yield (m^3/Mg)	Δ *	Max. Torque (%)
1	0.6	100	50	93.5 ± 1.1	+20.8%	52 ± 0.8
3	0.6	400	150	106.0 ± 1.5	+37.0%	67 ± 1.1
2	0.6	250	250	88.8 ± 1.2	+14.7%	59 ± 1.0
5	0.4	250	150	98.3 ± 1.0	+27.0%	51 ± 0.9
4	0.4	100	250	89.8 ± 1.1	+16.0%	46 ± 0.7
6	0.4	400	50	87.8 ± 2.0	+13.4%	39 ± 0.7
9	0.2	400	250	79.0 ± 1.5	+2.1%	46 ± 0.8
7	0.2	100	150	77.9 ± 2.4	+0.6%	45 ± 0.7
8	0.2	250	50	71.2 ± 1.1	−8.0%	43 ± 0.7

* Δ is relative to the reference T0 (77.4 m^3/Mg; 0.25 rpm, 350 s run, 150 s pause). Yield and maximum torque are given as the mean ± standard deviation of the two series ($n = 2$).

3.2. Main Effects and Factor Ranking

The Taguchi factor-means analysis (Table 5, Figure 1) identified rotational speed (X1) as the dominant factor, with a level-means range of 20.1 m^3/Mg—roughly double that of the pause time (X3, 9.9) and about four times that of the run time (X2, 4.8). The effect of speed was monotonic and positive: the highest speed (0.6 rpm) gave the highest mean yield (96.1 m^3/Mg) and the lowest speed (0.2 rpm) the lowest (76.0 m^3/Mg), corresponding to a strong and statistically significant positive correlation ($r = +0.80$, $n = 18$). An ordinary-least-squares regression of yield on rotational speed gave yield = 68.0 + 50.2·speed[rpm] ($R^2 = 0.64$, $p < 0.001$), i.e., an increase of about 5.0 m^3/Mg per 0.1 rpm. The increase was not uniform, however: most of it occurred between 0.2 and 0.4 rpm (about +16 m^3/Mg), and less between 0.4 and 0.6 rpm (about +4 m^3/Mg). The curvature was significant in the 18-run analysis (quadratic component, $p = 0.004$) but not in the conservative analysis of the setting means ($p = 0.23$), so the linear fit is used as a summary of a monotonic response that flattens toward the upper end of the tested range. Analysis of variance on the eighteen runs (Table 6) confirmed that rotational speed was by far the dominant factor ($F = 62.8$, $p < 0.001$), followed by pause time, which was also significant ($F = 15.7$, $p < 0.001$); run time, by contrast, was only marginally non-significant ($F = 3.7$, $p = 0.059$) and accounted for a small portion of the total variation. In terms of 95% confidence intervals (residual mean square, 11 df), the mean yield at 0.6 rpm exceeded that at 0.2 rpm by 20.1 ± 4.2 m^3/Mg, and the yield at the 150 s pause exceeded those at 50 s and 250 s by 9.9 ± 4.2 and 8.2 ± 4.2 m^3/Mg, respectively; the slope of the speed regression was 50.2 m^3/Mg per rpm (95% CI 30.4–70.0; 17.3–83.1 in the conservative analysis of the setting means). Speed, therefore, remains the primary lever for yield, with pause time a secondary factor, the robustness of which is discussed below. Because two-factor interactions are partially aliased with the main effects in the L9 array (Section 2.4), these main effects are averages over the levels of the other two factors and are interpreted accordingly. Expressed per unit of organic matter, using the measured feedstock characteristics, the same runs correspond to specific yields of about 220–330 m^3/Mg VS, with a regression of yield on speed of yield $_{VS}$ = 212.6 + 157.0·speed[rpm]. It should be

emphasized that, because a single mean TS and VS value was applied to all trials, this change in basis rescales the response by a constant factor and therefore leaves the coefficient of determination and the significance unchanged ($R^2 = 0.64$, $p < 0.001$); the organic-mass expression is provided for comparability with the literature, which reports specific methane or biogas yields per gram of VS [20,29], and not as an independent improvement of the model fit. Per-trial TS/VS measurements would be required to test whether normalizing organic load reduces the residual scatter.

Table 5. Level means of specific biogas yield from the 18 replicated runs; grand mean = 88.0 m^3/Mg.

Factor	Level −1 (m^3/Mg)	Level 0 (m^3/Mg)	Level +1 (m^3/Mg)	Range Δ (m^3/Mg)	ANOVA *p* (18 Runs/9 Means)	Rank
X1—speed	76.0	92.0	96.1	20.1	<0.001/0.068	1
X3—pause	84.2	94.1	85.9	9.9	<0.001/0.23	2
X2—run	87.1	86.1	90.9	4.8	0.059/0.55	3

Values are the level means, each the mean of the six runs sharing that level. No standard deviation is given for these level means because the spread of the six runs sharing a level mainly reflects the effects of the other two factors rather than experimental error. Experimental error is characterized by the standard error of a level mean derived from the ANOVA residual (Table 6), 1.3 m^3/Mg, and by the between-series repeatability standard deviation, 1.5 m^3/Mg (Section 3.2). The corresponding 95% confidence half-widths are ±2.9 m^3/Mg for a level mean and ±4.2 m^3/Mg for the difference between two level means of the same factor. ANOVA *p*-values are given for the 18 runs (pooled residual, 11 df) and for the nine setting means (unassigned column as error, 2 df; for speed, the linear component tested against the same error gives $p = 0.038$, and the regression of the nine setting means on speed $p = 0.009$); the rank orders factors by their level-means range (Δ).

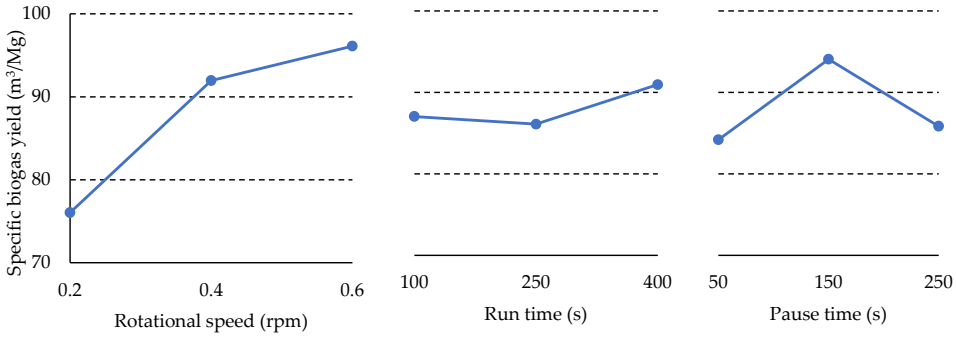


Figure 1. Main-effects plots for specific biogas yield.

Table 6. Analysis of variance (ANOVA) of specific biogas yield for the 18 replicated runs.

Source	Sum of Squares	df	*F*	*p*-Value	Significance
Rotational speed (X1)	1347.6	2	62.8	<0.001	***
Run time (X2)	79.5	2	3.7	0.059	n.s.
Pause time (X3)	335.9	2	15.7	<0.001	***
Residual (error)	118.0	11	—	—	—

Significance: *** $p < 0.001$. *F* values are tested against the pooled residual (11 df), which comprises the unassigned L9 column containing the aliased interactions (SS ≈ 97.7, 2 df) and the between-series pure error (SS ≈ 20.3, 9 df); lack-of-fit test: $F = 21.6$, $p < 0.001$. Including series as a block term (SS = 18.3, 1 df) did not change the conclusions (Section 3.2).

The two timing factors are far weaker than speed and differ in the strength of their evidence. The duplicate series were consistent—the pooled repeatability standard deviation was 1.5 m^3/Mg (coefficient of variation 1.7%)—but most of this between-series variation was a uniform shift: the second series gave a lower yield than the first at every setting (mean

difference 2.0 m^3/Mg, about 2%; paired *t*-test, $p < 0.001$), whereas the differences between settings were reproduced closely (standard deviation of the between-series differences 0.7 m^3/Mg). Because each series contained the complete L9 array, this shift is orthogonal to the factor effects and does not alter the level means or the factor sums of squares; with series included as a block term, the ANOVA conclusions were unchanged (speed: $F = 67.6$, $p < 0.001$; pause time: $F = 16.8$, $p < 0.001$; run time: $F = 4.0$, $p = 0.053$). Against the pooled residual (Table 6), pause time showed a significant intermediate optimum at 150 s ($F = 15.7$, $p < 0.001$). In contrast, run time showed only a marginally non-significant positive trend ($F = 3.7$, $p = 0.059$), with the longest run time (400 s) giving the highest mean yield. Two qualifications apply. First, the unassigned column of the L9 array, which contains the aliased two-factor interactions, was large relative to the between-series error (lack of fit: $F = 21.6$, $p < 0.001$), so interactions (e.g., speed × pause time) are probably not negligible. In this array, each two-factor interaction is split equally between the column of the third factor and the unassigned column; the speed × pause-time interaction, for example, is partly confounded with the run-time main effect. Interactions of the size indicated by the unassigned column (sum of squares of about 98) could therefore account for much or all of the apparent run-time effect (79.5) and for part of the pause-time effect (335.9), but not for the speed effect (1347.6), which is more than an order of magnitude larger. Second, because the two series are repeated operating periods of one reactor, the between-series error may underestimate the true experimental error. In the conservative analysis of the nine setting means, which has only 2 error degrees of freedom, none of the overall (2-df) factor effects reached significance (speed $p = 0.068$, pause time $p = 0.23$, run time $p = 0.55$; Table 5); however, the linear component of speed, which accounts for 90% of the speed sum of squares, remained significant ($F = 24.7$, $p = 0.038$), as did the regression of the nine setting means on speed ($r = +0.81$, $R^2 = 0.65$, $p = 0.009$). Speed is therefore the only factor whose effect is robust to both qualifications; the pause-time optimum at 150 s is plausible but should be regarded as indicative, and the run-time effect remains suggestive. Together, the two timing factors span about 5–10 m^3/Mg, against the roughly 20 m^3/Mg attributable to speed, so speed clearly dominates the response.

The direction of the speed effect—higher rotational speed yielding more biogas—is consistent with that reported for high-solids digestion [29] and contrasts with the behavior most often reported for dilute, wet systems, in which vigorous agitation tends to depress production [8,10,11]. A plausible explanation for this apparent divergence is the transport regime. In a 32–35% TS matrix, where yield stress and diffusional resistance are high [1,19], the process is likely to be limited by mass transfer rather than by reaction kinetics: hydrolysis proceeds at the particle surface. In contrast, acidogenesis and methanogenesis within the particle depend on diffusion, so more effective agitation would be expected to improve substrate–biomass contact and accelerate conversion. The present result is in direct agreement with Zhang et al. [29], who found, in batch dry digestion of sorghum stalks, that cumulative biogas increased with stirring speed up to 120 rpm, attributing the increase to the relief of this mass-transfer limitation. The magnitude of the effect observed here is substantial—a 26% difference between the mean yields at the lowest and highest tested speeds (76.0 versus 96.1 m^3/Mg)—which is consistent with a strong influence of mixing when transport, rather than kinetics, is rate-controlling.

The two studies can be compared on a common basis. Expressed as arm-tip linear velocity, the speed window tested here (7.0–20.9 cm/s, for 0.2–0.6 rpm at an effective radius of 3.32 m) lies below the lowest non-zero velocity used by Zhang et al. [29] (22 cm/s), whose yield increased monotonically up to 88 cm/s. The present reactor therefore appears to operate on the rising part of the same mixing-performance curve, where additional agitation still increases yield. Both studies thus show the same positive dependence of

yield on mixing intensity in high-solids digestion, and the present full-scale result extends that finding from batch laboratory conditions to a continuously operated commercial digester. This positive dependence is further supported by recent solid-state work. Nirunsin et al. [30] found that in pilot-scale solid-state digestion of sweet corn waste at 25% initial TS, the most frequent mixing and recirculation regime (every 3 h) produced the highest specific methane yield, whereas less frequent mixing reduced it. More broadly, the critical review of dry anaerobic digestion by Wang et al. [31] identifies mass-transfer limitation—arising from the high yield stress and restricted diffusion of a high-solids matrix—as the central constraint on performance, and notes that adequate mixing improves contact between substrate and biomass and can thereby boost biogas production. The present full-scale results are consistent with this mechanism, although they quantify the speed–yield relationship rather than the mechanism itself. Nonetheless, it should be noted that the benefit of more intensive mixing is not unconditional. In an intermittently mixed vinasse digester, higher mixing speeds increased biogas production but also caused larger fluctuations, as volatile fatty acids accumulated in acidic zones of the settled sludge were released into the liquid on mixing [13]; the benefit observed here is therefore specific to a transport-limited regime in which no such destabilization occurred (Section 3.4).

The very low absolute speeds are consistent with this transport-limited interpretation. Because the tested window (0.2–0.6 rpm) lies well below the range in which hydrodynamic shear damages microbial flocs—a phenomenon reported near 1500 rpm in dilute systems, and even there affecting mainly start-up rather than steady state [9,15]—the detrimental, shear-related effects of mixing are not expected to appear here. What is more likely to vary across the tested range is the degree to which the dense matrix is renewed at the reaction front, which would increase with speed. The weak influence of run time fits the same picture: once the shaft has swept the chamber and refreshed the substrate–biomass contact, the immediate mass-transfer requirement is met [19,29], so extending the run at a given speed adds energy without a commensurate yield gain, whereas raising the speed itself renews contact more intensively and does increase yield.

The mixing action of this reactor is consistent with the transport-limited interpretation. In this digester, agitation is provided by a slow horizontal shaft that acts on the stiff 32–35% TS mass largely by kneading, continuously folding fresh and digesting material together rather than generating the high hydrodynamic shear of a fast impeller in a dilute slurry [32]. Faster rotation increases the frequency of this folding and, hence, the rate at which substrate is presented to the biomass at the reaction front; in a diffusion-limited matrix, this would be expected to translate into higher conversion and gas yield. That the digester remained fully stable at every setting—with uniformly low outlet VFAs and FOS/TAC well below the warning threshold—indicates that the additional mixing did not provoke any adverse response, so the yield gain is unlikely to reflect a change in process health and is consistent with, although not proof of, a relief of mass-transfer limitation. This mechanism is specific to transport-limited high-solids operation; in a well-mixed or dilute system, where mass transfer is already satisfied, the same increase in speed would not be expected to increase yield and could, at much higher shear rates, become detrimental [9,15].

The observed strong positive dependency of biogas yield on agitator rotational speed can be further elucidated by the distinct rheological behavior of high-solids digestate. As reviewed by Wang et al. [31] and Gao et al. [1], high-solids digestates in this TS range exhibit non-Newtonian, pseudoplastic behavior characterized by a high yield stress. At low rotational speeds (e.g., 0.2 rpm), the mechanical energy imparted by the horizontal shaft may be insufficient to overcome the structural yield stress throughout the reactor bulk, leaving stagnant or poorly mixed zones [1,31]. A plausible interpretation is that increasing the rotational speed to 0.6 rpm improves spatial substrate turnover and reduces localized

mass-transfer resistances, while remaining well below the shear levels associated with cell disruption [9,31]. It should be emphasized that these mechanisms—reduced dead zones, matrix fluidization, and enhanced mass transfer—are offered as interpretations consistent with the data and the cited rheological studies; they were not measured directly in this work, and would require flow-field or tracer characterization to confirm.

3.3. Mixing Energy

The maximum agitator torque increased with rotational speed (Figure 2), in parallel with the specific biogas yield of the individual runs (Figure 3). At 0.6 rpm, the maximum torque averaged 59% of nominal torque, compared with about 45% at 0.4 and 0.2 rpm. Torque alone, however, is not a measure of energy consumption: the shaft power is proportional to the product of torque and angular velocity, and the energy demand additionally depends on the fraction of time the agitator runs (duty cycle) and on the drive efficiency. Because speed, run time, and pause time are themselves experimental factors, the relative mixing-energy index E_{rel} (Section 2.4) was calculated for each setting (Table 7). E_{rel} differed about eightfold between the settings (0.12–1.00), and the yield-maximizing set-point (Trial 3: 0.6 rpm, 400 s run, 150 s pause; +37% versus the reference) also had the highest index. The yield-maximizing operating point, therefore, differs from the energy-efficient ones: only Trials 7, 4, 5, and 3 were not outperformed by another setting with both a higher yield and a lower E_{rel} (Table 7), i.e., these four settings form the Pareto front of yield versus mixing energy. Of these, Trial 4 (0.4 rpm, 100 s run, 250 s pause) reached 89.8 m^3/Mg at E_{rel} = 0.18, and Trial 5 (0.4 rpm, 250 s run, 150 s pause) reached 98.3 m^3/Mg at E_{rel} = 0.44, i.e., 93% of the maximum yield at less than half of the mixing-energy index of Trial 3. Selecting an operating point, therefore, requires weighing the value of the additional biogas against the extra electricity consumed by the agitator. Because the electrical input of the drive was not metered, this trade-off can be bounded but not resolved with the present data.

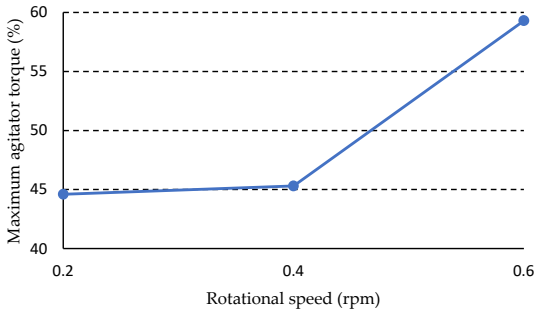


Figure 2. Main-effects plots for maximum agitator torque.

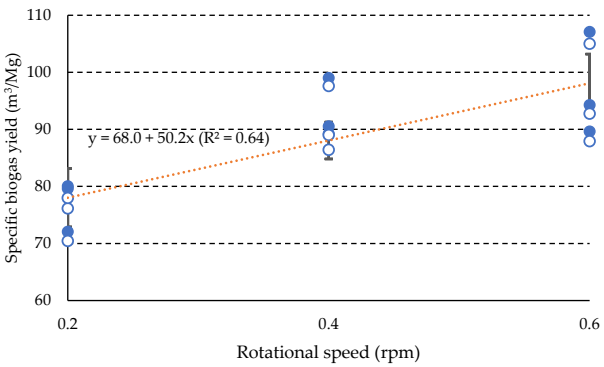


Figure 3. Specific biogas yield versus rotational speed for the 18 runs (filled circles: first series; open circles: second series), with the linear regression (dotted line); vertical bars show the 95% confidence interval of the regression line at the tested speeds.

Table 7. Duty cycle, maximum torque, relative mixing-energy index (E_{rel}), and specific biogas yield of the nine settings.

Trial	X1 (rpm)	X2/X3 (s)	Duty Cycle (%)	Max. Torque (%)	E_{rel} (-)	Yield (m^3/Mg)
3 [a]	0.6	400/150	72.7	67	1.00	106.0
1	0.6	100/50	66.7	52	0.71	93.5
2	0.6	250/250	50.0	59	0.61	88.8
6	0.4	400/50	88.9	39	0.47	87.8
5 [a]	0.4	250/150	62.5	51	0.44	98.3
4 [a]	0.4	100/250	28.6	46	0.18	89.8
8	0.2	250/50	83.3	43	0.25	71.2
9	0.2	400/250	61.5	46	0.19	79.0
7 [a]	0.2	100/150	40.0	45	0.12	77.9

Duty cycle = $t_{run}/(t_{run} + t_{pause})$; $E_{rel} = (\tau/100)\cdot N\cdot$duty cycle, normalized to Trial 3; E_{rel} is proportional to the time-averaged shaft power if the operating torque is proportional to the maximum recorded torque and the drive efficiency is constant. Torque and yield are measured values; E_{rel} is a derived index, not a metered energy consumption. [a] Non-dominated settings: no other setting gave a higher yield at a lower E_{rel}.

Only the yields and torque values are measured; the energy figures below are illustrative estimates based on stated assumptions, because the electrical input of the agitator drive was not metered. Future studies should incorporate direct power analyzers on the agitator drive to establish net energy balances with high temporal resolution.

To evaluate the net energy implications of the yield-maximizing set-point (0.6 rpm, 400 s run, 150 s pause—the best combination tested), the additional electricity that could be generated from the extra biogas was benchmarked against the agitator's mixing-energy index. Based on an average methane content of 54%, a methane lower heating value of about 10 kWh/m^3 CH_4, and a typical combined heat and power (CHP) electrical efficiency of 40% [3,5], the yield increase from the reference 77.4 m^3/Mg to the optimum mean of 106.0 m^3/Mg feedstock (Table 4) generates an additional electricity output of approximately 61.8 kWh per Mg of treated biowaste ($(106.0 - 77.4) \times 0.54 \times 10 \times 0.40$). At a mean daily throughput of 43 Mg/d, this corresponds to a gross daily electrical energy gain of approximately 2656 kWh/d, or about 110 kW on average. Whether this gain outweighs the additional mixing energy depends on the absolute power of the agitator drive, which can be expressed as break-even values. Relative to Trial 5, the yield-maximizing setting yields about 30 kW of additional average electrical output, while 56% of its mixing energy is additional (E_{rel} = 1.00 versus 0.44); moving from Trial 5 to Trial 3 is therefore net-positive only if the time-averaged electrical demand of the agitator at Trial 3 is below about 53 kW. These estimates neglect the CHP unit's heat output and the uncertainty in yield differences, and should be confirmed by metered energy balances.

These figures place the mixing-energy penalty of higher-speed operation in context. High-solids digesters inherently require substantial mechanical power to overcome apparent viscosity and yield stress, so raising the rotational speed increases the agitator's electrical demand. Agitation is a leading parasitic load in biogas plants [5], and optimizing the stirring regime together with the digester temperature has been shown at full scale to raise the specific electricity yield while reducing internal energy use [4]; at laboratory scale, intermittent operation saved about 29% of the mixing power without loss of methane yield [23]. Unlike those wet-digestion studies, the present high-solids digester did not show a win–win optimum: the setting with the highest yield also had the highest mixing-energy index, and the setting with the lowest index (Trial 7) gave virtually no gain over the reference. Compared with the 11.7% gain in specific electricity yield reported for combined stirring and temperature management in conventional wet digestion [4], the 37% maximum increase in

specific biogas yield observed in this high-solids trial (relative to a single reference period) indicates that rheology-aware mixing management is an important optimization lever for dry digestion. However, its net benefit has to be confirmed by metered energy balances.

3.4. Process Stability

Across all runs, the digester remained well-buffered and stable (Figure 4). The outlet FOS/TAC ratio remained within 0.13–0.17, well below the commonly regarded early warning of acidification, and showed no adverse trend throughout the campaign. The individual volatile fatty acids, measured at the inlet, middle, and outlet, confirm this stability in more detail than the FOS/TAC ratio alone. Acetic acid—the dominant VFA and the immediate methanogenic precursor—entered the chamber at 813–1172 mg/kg and decreased to 1–17 mg/kg at the outlet in every trial, i.e., a net decrease in concentration of about 99.5% (98.5–99.9%) along the chamber. Because VFAs are produced and consumed simultaneously, this net decrease shows that consumption exceeded production by the outlet; it is not an overall degradation efficiency. Propionic acid, the most inhibition-sensitive intermediate, fell from 10–53 mg/kg at the inlet to ≤10 mg/kg at the outlet, and butyric acid from ≤17 to ≤5 mg/kg; the branched and higher acids (iso-butyric, valeric, and iso-valeric) remained at or near the 1 mg/kg detection limit throughout. Critically, the near-complete net removal of VFAs and the absence of any propionate buildup were observed across the full range of agitator settings, including the highest-speed runs, indicating that the acetogenic-to-methanogenic handoff remained healthy irrespective of the mixing regime and that no VFA accumulation occurred. Ammonium nitrogen (3.8–4.2 g/kg) remained within a non-inhibitory range. This stability is notable because high-solids digestion is generally more prone to local VFA accumulation and mass-transfer-limited inhibition than wet digestion [1,19]; its absence here is consistent with adequate contact without over-shearing at these settings.

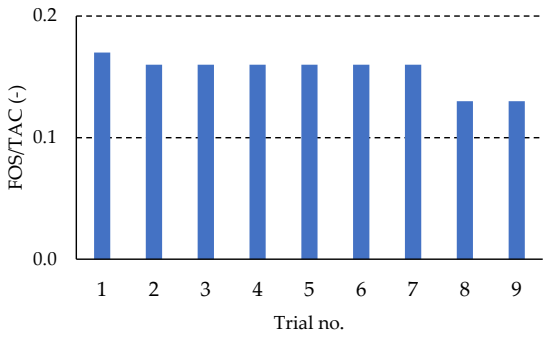


Figure 4. Process-stability indicator across trials: outlet FOS/TAC ratio.

The persistence of full stability is analytically important. Because acidification was never limiting, the observed yield differences are unlikely to be explained by differences in process health. Stable FOS/TAC does not, by itself, prove that mixing caused the yield differences. Still, it rules out acid inhibition as a competing explanation. It is therefore consistent with a mixing-related effect, which, in some laboratory studies, is confounded by VFA inhibition at high organic loading [8,17].

3.5. Yield-Maximizing Setting, Confirmation, and Limitations

Under the "larger-the-better" criterion, the additive model indicated the optimum combination X1 = 0.6 rpm, X2 = 400 s, X3 = 150 s, with a predicted specific yield of 105.1 m^3/Mg. An independent confirmation run at these settings yielded 104.4 m^3/Mg, reproducing the prediction to within about 1%; because this combination coincides with Trial 3 of the ar-

ray (106.0 m^3/Mg), the run confirms the reproducibility of the yield-maximizing setting rather than validating the model for an untested combination. The 95% prediction interval for a single new run at these settings, based on the residual mean square of the 18-run ANOVA (11 df) and the variance of the additive prediction (7/18 of the error variance), is 105.1 ± 8.5 m^3/Mg (96.6–113.6 m^3/Mg); with the between-series error (9 df), it narrows to 105.1 ± 4.0 m^3/Mg (101.1–109.1 m^3/Mg). The confirmation result lies within both intervals, i.e., within the expected experimental variability, although a single run cannot characterize the reproducibility of the prediction. The optimum combines the highest speed, the longest run time, and the intermediate pause time, with speed by far the largest term and pause time a secondary contributor; the run-time contribution, though pointing to the longest setting, is statistically marginal. The simple speed-only regression provides a lower-bound estimate that ignores the two timing terms: at 0.6 rpm, yield = 68.0 + 50.2 × 0.6 = ca. 98 m^3/Mg, a gap to the additive prediction that reflects the secondary contributions of pause time and run time. This combination is the yield-maximizing setting within the investigated range (0.2–0.6 rpm); it should be read as the best tested speed rather than a global optimum, since higher speeds were not evaluated. It is not, however, the energy-efficient setting: among the Pareto-optimal (non-dominated) settings (Section 3.3, Table 7), Trials 4 and 5 (0.4 rpm) retain 85–93% of the maximum yield at 18–44% of its mixing-energy index, whereas Trial 7 (0.2 rpm), despite the lowest index, gives virtually no gain over the reference; the choice between Trials 4, 5, and 3 depends on the drive power and on the value of electricity.

Several limitations temper these conclusions. First, the specific yield was normalized to fresh feedstock mass using common mean TS and VS values; because per-trial substrate composition and biodegradability were not measured and feedstock TS varied considerably (44.1 ± 10.4%), part of the variation in yield per unit fresh mass may reflect differences in the amount of volatile solids fed rather than mixing. The absence of a correlation between OLR and yield (Section 3.1) argues against a strong loading effect, but it cannot exclude compositional effects. Second, because the settings were applied sequentially on one reactor, in an operator-determined order within each series, temporal effects (seasonal feedstock shifts, slow microbial adaptation) cannot be separated from the treatment effects with certainty; the close agreement between the two non-adjacent replicate series (repeatability SD 1.5 m^3/Mg) argues against a strong campaign drift, but the second series gave uniformly lower yields than the first (by about 2%; Section 3.2), indicating a small temporal drift; being uniform across settings and orthogonal to the design, it did not bias the factor effects, but drift within a series cannot be excluded. For the same reason, the gains relative to the pre-experiment reference (T0), which was a single, unreplicated operating period, are less certain than the comparisons between settings within the design. The regression and ANOVA assume independent, homoscedastic residuals; the residuals showed no significant departure from normality (Shapiro–Wilk $W = 0.91$, $p = 0.07$) and no heteroscedasticity (Levene's test across speed levels, $p = 0.99$; Bartlett's test across settings, $p = 0.99$; Spearman correlation between absolute residuals and fitted values, $\rho = 0.10$, $p = 0.71$), but the temporal ordering means residuals are not guaranteed to be fully independent, which is why the conservative analysis of setting means was also reported. Although the design was replicated, allowing the factor effects to be established by ANOVA, the L9 design does not resolve two-factor interactions, which are partially aliased with the main effects, and the significant lack of fit indicates that such interactions are present. Electrical power was not metered, and E_{rel} is based on the maximum rather than the time-averaged torque, so E_{rel} and the energy figures are relative or illustrative. The optimum is specific to this high-solids, horizontal-shaft OFMSW digester and to the tested speed window (0.2–0.6 rpm); the general lesson (that yield rises monotonically with speed over this range and that the highest tested speed gives the highest yield) is more transferable than the specific num-

bers. The finding should not be extrapolated to wet, kinetically limited systems, where vigorous mixing can instead depress yield; the direction of the speed effect in a digester is contingent on whether mass transfer or reaction kinetics is rate-limiting, and the present positive dependence is consistent with a mass-transfer-limited high-solids regime. Future work should include direct energy metering; per-period feedstock TS/VS measurements; characterization of digestate rheology as a function of TS; spatially resolved or microbial community measurements to test the proposed micro-environment mechanism directly; and, ideally, extending the speed window below 0.2 rpm to locate the point at which insufficient mixing begins to impair contact. Furthermore, while the L9 orthogonal matrix with duplicate trials effectively resolved main factor effects and repeatability, full quantification of potential two-factor interactions (e.g., speed × pause time) would require a complete factorial or response surface design.

4. Conclusions

A full-scale experiment on a municipal high-solids (32–35% TS) biowaste digester showed that agitator operation has a large and controllable effect on specific biogas yield, which varied by a factor of 1.5 across the nine settings (each run in two series) without intentional changes to feedstock or loading. Rotational speed was the dominant parameter, with yield increasing monotonically as speed increased, most strongly between 0.2 and 0.4 rpm ($r = +0.80$; yield = 68.0 + 50.2·speed[rpm], $R^2 = 0.64$, $p < 0.001$, $n = 18$), and its linear component remained significant in a conservative analysis of the nine setting means. Pause time was a secondary factor whose effect was less robust, while run time was only marginally non-significant; because interactions are aliased with the main effects in the L9 design, these main effects should be read as averages over the levels of the other factors. The yield-maximizing setting (0.6 rpm, 400 s run, 150 s pause) increased yield by 37% over the pre-experiment reference (a single, unreplicated operating period), and a confirmation run agreed with the additive-model prediction to within 1%. Because the mixing-energy index (torque × speed × duty cycle) also peaked at this setting, the yield-maximizing setting differs from the energy-efficient settings (0.4 rpm, Trials 4 and 5), and whether the additional biogas outweighs the additional mixing energy can only be established by metered energy balances. The digester remained fully stable throughout, indicating that the gains are unlikely to arise from process recovery; relief of mass-transfer limitation is the most plausible interpretation, though it was not demonstrated directly. For this class of high-solids horizontal-shaft digester, the results give operators a clear, low-cost lever—raising the agitator speed toward the upper end of the tested range (up to 0.6 rpm) when yield is the priority, or operating at 0.4 rpm (Trials 4 and 5) when mixing energy matters—and they extend the largely wet-system mixing literature into the high-solids regime, where the dependence of yield on mixing intensity may differ from that commonly reported for wet systems.

Author Contributions: Conceptualization, P.S.; methodology, P.S. and W.C.; formal analysis, P.S.; investigation, A.U., M.J. and M.W.; resources, P.S. and W.C.; data curation, P.S. and M.J.; writing—original draft preparation, P.S.; writing—review and editing, W.C. and A.U.; visualization, M.W. and M.J.; supervision, P.S. All authors have read and agreed to the published version of the manuscript.

Funding: This research received no external funding.

Data Availability Statement: The data presented in this study are available on request from the corresponding authors.

Conflicts of Interest: The authors declare no conflicts of interest.

References

1. Gao, Q.; Li, L.; Wang, K.; Zhao, Q. Mass Transfer Enhancement in High-Solids Anaerobic Digestion of Organic Fraction of Municipal Solid Wastes: A Review. *Bioengineering* **2023**, *10*, 1084. [CrossRef] [PubMed]
2. Lamolinara, B.; Pérez-Martínez, A.; Guardado-Yordi, E.; Guillén Fiallos, C.; Diéguez-Santana, K.; Ruiz-Mercado, G.J. Anaerobic Digestate Management, Environmental Impacts, and Techno-Economic Challenges. *Waste Manag*. **2022**, *140*, 14–30. [CrossRef] [PubMed]
3. Havukainen, J.; Uusitalo, V.; Niskanen, A.; Kapustina, V.; Horttanainen, M. Evaluation of Methods for Estimating Energy Performance of Biogas Production. *Renew. Energy* **2014**, *66*, 232–240. [CrossRef]
4. Önen, S.; Nsair, A.; Kuchta, K. Innovative Operational Strategies for Biogas Plant Including Temperature and Stirring Management. *Waste Manag. Res*. **2019**, *37*, 237–246. [CrossRef] [PubMed]
5. Naegele, H.-J.; Lemmer, A.; Oechsner, H.; Jungbluth, T. Electric Energy Consumption of the Full Scale Research Biogas Plant "Unterer Lindenhof": Results of Longterm and Full Detail Measurements. *Energies* **2012**, *5*, 5198–5214. [CrossRef]
6. Tian, L.; Zou, D.; Yuan, H.; Wang, L.; Zhang, X.; Li, X. Identifying Proper Agitation Interval to Prevent Floating Layers Formation of Corn Stover and Improve Biogas Production in Anaerobic Digestion. *Bioresour. Technol*. **2015**, *186*, 1–7. [CrossRef] [PubMed]
7. Subramanian, B.; Pagilla, K.R. Anaerobic Digester Foaming in Full-Scale Cylindrical Digesters—Effects of Organic Loading Rate, Feed Characteristics, and Mixing. *Bioresour. Technol*. **2014**, *159*, 182–192. [CrossRef] [PubMed]
8. Lindmark, J.; Thorin, E.; Bel Fdhila, R.; Dahlquist, E. Effects of Mixing on the Result of Anaerobic Digestion: Review. *Renew. Sustain. Energy Rev*. **2014**, *40*, 1030–1047. [CrossRef]
9. Hoffmann, R.A.; Garcia, M.L.; Veskivar, M.; Karim, K.; Al-Dahhan, M.H.; Angenent, L.T. Effect of Shear on Performance and Microbial Ecology of Continuously Stirred Anaerobic Digesters Treating Animal Manure. *Biotechnol. Bioeng*. **2008**, *100*, 38–48. [CrossRef] [PubMed]
10. Singh, B.; Szamosi, Z.; Siménfalvi, Z. Impact of Mixing Intensity and Duration on Biogas Production in an Anaerobic Digester: A Review. *Crit. Rev. Biotechnol*. **2020**, *40*, 508–521. [CrossRef] [PubMed]
11. Kariyama, I.D.; Zhai, X.; Wu, B. Influence of Mixing on Anaerobic Digestion Efficiency in Stirred Tank Digesters: A Review. *Water Res*. **2018**, *143*, 503–517. [CrossRef] [PubMed]
12. Kaparaju, P.; Buendia, I.; Ellegaard, L.; Angelidaki, I. Effects of Mixing on Methane Production During Thermophilic Anaerobic Digestion of Manure: Lab-Scale and Pilot-Scale Studies. *Bioresour. Technol*. **2008**, *99*, 4919–4928. [CrossRef] [PubMed]
13. Caillet, H.; Madyira, D.M.; Adelard, L. Study of the Performances of a Vinasse Mesophilic Anaerobic Digester Behavior Submitted to Intermittent Mixing: Monitoring of the Physicochemical Properties of the Digestate and Local Samples of the Digester. *Bioresour. Technol. Rep*. **2021**, *16*, 100837. [CrossRef]
14. Singh, B.; Kovács, K.L.; Bagi, Z.; Petrik, M.; Szepesi, G.L.; Siménfalvi, Z.; Szamosi, Z. Significance of Intermittent Mixing in a Mesophilic Anaerobic Digester. *Fermentation* **2022**, *8*, 518. [CrossRef]
15. Lebranchu, A.; Delaunay, S.; Marchal, P.; Blanchard, F.; Pacaud, S.; Fick, M.; Olmos, E. Impact of Shear Stress and Impeller Design on the Production of Biogas in Anaerobic Digesters. *Bioresour. Technol*. **2017**, *245*, 1139–1147. [CrossRef] [PubMed]
16. Singh, B.; Kovács, K.L.; Bagi, Z.; Nyári, J.; Szepesi, G.L.; Petrik, M.; Siménfalvi, Z.; Szamosi, Z. Enhancing Efficiency of Anaerobic Digestion by Optimization of Mixing Regimes Using Helical Ribbon Impeller. *Fermentation* **2021**, *7*, 251. [CrossRef]
17. Ghanimeh, S.A.; Al-Sanioura, D.N.; Saikaly, P.E.; El-Fadel, M. Correlation Between System Performance and Bacterial Composition Under Varied Mixing Intensity in Thermophilic Anaerobic Digestion of Food Waste. *J. Environ. Manag*. **2018**, *206*, 472–481. [CrossRef] [PubMed]
18. Latha, K.; Velraj, R.; Shanmugam, P.; Sivanesan, S. Mixing Strategies of High Solids Anaerobic Co-Digestion Using Food Waste with Sewage Sludge for Enhanced Biogas Production. *J. Clean. Prod*. **2019**, *210*, 388–400. [CrossRef]
19. Li, L.; Wang, K.; Sun, Z.; Zhao, Q.; Zhou, H.; Gao, Q.; Jiang, J.; Mei, W. Effect of Optimized Intermittent Mixing during High-Solids Anaerobic Co-Digestion of Food Waste and Sewage Sludge: Simulation, Performance, and Mechanisms. *Sci. Total Environ*. **2022**, *842*, 156882. [CrossRef] [PubMed]
20. Rocamora, I.; Wagland, S.T.; Villa, R.; Simpson, E.W.; Fernández, O.; Bajón-Fernández, Y. Dry Anaerobic Digestion of Organic Waste: A Review of Operational Parameters and Their Impact on Process Performance. *Bioresour. Technol*. **2020**, *299*, 122681. [CrossRef] [PubMed]
21. Kress, P.; Nägele, H.-J.; Oechsner, H.; Ruile, S. Effect of Agitation Time on Nutrient Distribution in Full-Scale CSTR Biogas Digesters. *Bioresour. Technol*. **2018**, *247*, 1–6. [CrossRef] [PubMed]
22. Lemmer, A.; Naegele, H.-J.; Sondermann, J. How Efficient Are Agitators in Biogas Digesters? Determination of the Efficiency of Submersible Motor Mixers and Incline Agitators by Measuring Nutrient Distribution in Full-Scale Agricultural Biogas Digesters. *Energies* **2013**, *6*, 6255–6273. [CrossRef]
23. Kowalczyk, A.; Harnisch, E.; Schwede, S.; Gerber, M.; Span, R. Different Mixing Modes for Biogas Plants Using Energy Crops. *Appl. Energy* **2013**, *112*, 465–472. [CrossRef]

24. Singh, B.; Szamosi, Z.; Siménfalvi, Z. State of the Art on Mixing in an Anaerobic Digester: A Review. *Renew. Energy* **2019**, *141*, 922–936. [CrossRef]
25. Rice, E.W.; Baird, R.B.; Eaton, A.D.; Clesceri, L.E. (Eds.) *Standard Methods for the Examination of Water and Wastewater*, 22nd ed.; American Public Health Association (APHA): Washington, DC, USA; American Water Works Association (AWWA): Washington, DC, USA; Water Environment Federation (WEF): Washington, DC, USA, 2012.
26. Sidi Habib, S.; Torii, S.; Kavitha Mol, S.; Charivuparampil Achuthan Nair, A. Optimization of the Factors Affecting Biogas Production Using the Taguchi Design of Experiment Method. *Biomass* **2024**, *4*, 687–703. [CrossRef]
27. Mehryar, E.; Ding, W.; Hemmat, A.; Hassan, M.; Talha, Z.; Kafashan, J.; Huang, H. Modeling and Multiresponse Optimization for Anaerobic Co-digestion of Oil Refinery Wastewater and Chicken Manure by Using Artificial Neural Network and the Taguchi Method. *BioMed Res. Int.* **2017**, *2017*, 2036737. [CrossRef] [PubMed]
28. Montgomery, D.C. *Design and Analysis of Experiments*, 9th ed.; John Wiley & Sons: Hoboken, NJ, USA, 2017.
29. Zhang, Z.; Chang, S.; Zhao, S.; Liu, P.; Qian, Y.; Li, W. Impact of Mechanical Stirring and Percolate Recirculation on the Performances of Dry Anaerobic Digestion. *Fermentation* **2023**, *9*, 848. [CrossRef]
30. Nirunsin, R.; Saipa, S.; Sawatdeenarunat, C. Solid-State Anaerobic Digestion of Sweet Corn Waste: The Effect of Mixing and Recirculation Interval. *Int. J. Renew. Energy Dev.* **2024**, *13*, 1035–1043. [CrossRef]
31. Wang, Z.; Hu, Y.; Wang, S.; Wu, G.; Zhan, X. A Critical Review on Dry Anaerobic Digestion of Organic Waste: Characteristics, Operational Conditions, and Improvement Strategies. *Renew. Sustain. Energy Rev.* **2023**, *176*, 113208. [CrossRef]
32. Deublein, D.; Steinhauser, A. *Biogas from Waste and Renewable Resources: An Introduction*, 2nd ed.; Wiley-VCH: Weinheim, Germany, 2011.

Disclaimer/Publisher's Note: The statements, opinions and data contained in all publications are solely those of the individual author(s) and contributor(s) and not of MDPI and/or the editor(s). MDPI and/or the editor(s) disclaim responsibility for any injury to people or property resulting from any ideas, methods, instructions or products referred to in the content.